





# Predicting individual decision-making responses based on the functional connectivity of resting-state EEG

Yajing Si<sup>1,2</sup> , Lin Jiang<sup>1,2</sup>, Qin Tao<sup>1,2</sup>, Chunli Chen<sup>1,2</sup>, Fali Li<sup>1,2</sup> , Yuanling Jiang<sup>1,2</sup>, Tao Zhang<sup>1,2,3</sup> , Xianyu Cao<sup>1,2</sup>, Feng Wan<sup>4</sup> , Dezhong Yao<sup>1,2</sup> and Peng Xu<sup>1,2,5</sup>

<sup>1</sup> The Clinical Hospital of Chengdu Brain Science Institute, MOE Key Lab for Neuroinformation, University of Electronic Science and Technology of China, Chengdu 611731, People's Republic of China

<sup>2</sup> School of Life Science and Technology, a Center for Information in BioMedicine, University of Electronic Science and Technology of China, Chengdu 611731, People's Republic of China

<sup>3</sup> Xihua University, Chengdu 610039, People's Republic of China

<sup>4</sup> Faculty of Science and Technology, University of Macau, Macau 999078, People's Republic of China

E-mail: [xupeng@uestc.edu.cn](mailto:xupeng@uestc.edu.cn)

Received 15 April 2019, revised 25 July 2019

Accepted for publication 8 August 2019

Published 30 October 2019



## Abstract

**Objective.** Despite increasing evidence revealing the relationship between task-related brain activity and decision-making, the association between resting-state functional connectivity and decision-making remains unknown. **Approach.** In this study, we investigated the potential relationship between the network revealed in the resting-state electroencephalogram (EEG) and decision responses and further predicted individuals' acceptance rates during the ultimatum game (UG) based on the functional connectivity revealed in the resting-state EEG. **Main results.** The results of this study demonstrated a significant relationship between the resting-state frontal-occipital connectivity and the UG acceptance rate in the alpha band. Increased acceptance rates were accompanied by a larger clustering coefficient and global and local efficiency as well as a shorter characteristic path length. Compared to the low-acceptance group, the high-acceptance group exhibited stronger frontal-occipital linkages. Finally, a multiple linear regression model based on the resting-state EEG network properties was adopted to predict the acceptance rates when subjects made their decision in the UG task. **Significance.** Together, the findings of this study may deepen our knowledge of decision-making and provide a potential physiological biomarker to predict the decision-making responses of subjects.

**Keywords:** decision-making, resting-state, brain network, response prediction

(Some figures may appear in colour only in the online journal)

## 1. Introduction

To make a decision, individuals will take varied information into account, weigh the options, and finally come to a conclusion (Neuberta *et al* 2015). The response of decision-making is linked not only to economic and social progress but also to almost all areas of daily life (Kaltwasser *et al* 2016, Tremblay

*et al* 2017). Individuals with efficient decision-making ability appear to experience obvious network connectivity between the anterior insula and frontal lobe when integrating emotional and cognitive information (Sanfey *et al* 2003). By contrast, a deficit in decision-making may be the result of impairments of cognitive brain functions, including cognitive control (Waskom *et al* 2016), monitor of action (Amodio and Frith 2006), attention (Dodds *et al* 2010) and goal maintenance (Sanfey *et al* 2003).

<sup>5</sup> Author to whom any correspondence should be addressed.

In studies related to social science, decision-making is usually investigated by adopting the ultimatum game (UG) (Kirk *et al* 2011, Wang *et al* 2017), which includes a proposer and a responder in a typical bargaining situation. Various studies have indicated that UGs can simulate decision-making well and reveal the subject's behavior when facing unfair conditions (Horat *et al* 2017, Peterburs *et al* 2017). In the UG task, the proposer is responsible for dividing money into two shares; based on the proposed offer, the responder will then decide to accept or reject this offer. When the responder accepts the offer, both players receive the money; if the offer is rejected, both of them earn nothing. The acceptance rate of the offer is often used to characterize the UG task performance of individual subjects (Wang *et al* 2017), since the acceptance rate varies across individuals. A relatively low acceptance rate implies that the individual prefers fairness by making a rejection to punish the proposer's unfair behavior (Yamagishi *et al* 2009).

Heretofore, previous studies have revealed the neural mechanisms underlying economic decision-making during decision-making tasks and have demonstrated the crucial roles of the anterior cingulate cortex (ACC) (Suzuki *et al* 2012), ventromedial prefrontal cortex (Bartra *et al* 2013), the dorsolateral prefrontal cortex (Krain *et al* 2006) and the insula (Critchley *et al* 2000) in decision-making. Physiologically, the activation of the prefrontal cortex may relate to the comparison of costs and benefits of offers by evaluating the difference between neural signatures of anticipated benefits and costs from the ventral striatum and amygdala (Basten *et al* 2010). When an individual rejects unfair offers, the frontal cortex also plays a role in connecting the parietal and occipital cortices (Si *et al* 2018). Meanwhile, the generation of a decision is also involved in emotion, which is mostly based on the integrated information induced by both the anterior insula and prefrontal cortex, which represent the two demands of the decision task (i.e. the emotional goal and the cognitive goal) (Sanfey *et al* 2003). The blood oxygen level-dependent (BOLD) activity of the anterior insula has been shown to consistently increase with the degree of difficulty of the decision-making (Lamichhane *et al* 2016).

Despite decision-making versus task-related network connectivity, the relationship between the functional brain network at rest and decision-making has not yet been investigated. In fact, the brain at rest works and is characterized by a specific network mode incorporating different regions (Kounios *et al* 2008, Zhang *et al* 2014). Theoretically, the brain network at rest can characterize the intrinsic allocation of brain resources and is helpful to predict individual task performance (Northoff *et al* 2010, Xu *et al* 2014, Tian *et al* 2017a). Recently, the potential relationship between the resting-state brain network and brain cognition has been widely investigated (Brokaw *et al* 2016, Falahpour *et al* 2018). For example, the high temporal variability of the resting network connectivity among brain regions including the lateral prefrontal cortex, parahippocampal gyrus and precuneus was demonstrated to be significantly related to high verbal creativity (Sun *et al* 2018). Li *et al.* investigated the relationship between P3 and resting-state network topology and showed that larger P3 amplitudes were

correlated with a more efficient resting-state brain network (Li *et al* 2015). For motor imagery, the previous study also demonstrated that an efficient resting-state electroencephalogram (EEG) network facilitates motor imagery performance in the task (Zhang *et al* 2015). The resting-state functional connectivity in decision-making networks, such as the frontoparietal network and dorsal anterior cingulate-anterior insular cortex network, has also been shown to be related to the discounting rate of subjects (an index of impulsivity) and can predict the economic decision behavior in a delay discount task (Li *et al* 2013).

Rather than the isolated operations of distributed regions, large-scale networks among multiple areas are demonstrated to greatly contribute to human cognition (Buschman and Miller 2007, Dixon *et al* 2017, Zhang 2018). Previous studies have demonstrated a replicable pattern of brain activity in decision-making (Wang *et al* 2016, Shao *et al* 2016). The frontal lobe plays a crucial role in the deliberation process of decision-making, which is accomplished by sending information to other related regions, including the ACC, sensorimotor area and insula (Sanfey *et al* 2003, Kim and Lee 2011, Suzuki *et al* 2012). More recently, our knowledge of decision-making topology has also denoted the importance of various neural networks for decision-making (Paulus *et al* 2001). In this study, we hypothesized that the resting-state brain network may be used to infer the performance of subjects when making decisions. Aiming to validate our hypothesis, we collected resting and task EEG data sets when subjects participated in the UG task and utilized brain network analysis to investigate the potential relationship between brain network connectivity at rest and decision-making, from which a model is established to predict individual performance during decision-making.

## 2. Materials and methods

### 2.1. Participants

The experimental protocol was approved by the Institution Research Ethics Board of the University of Electronic Science and Technology of China (UESTC). Eighteen right-handed participants were recruited from the student population of the UESTC. Written informed consent was obtained after the procedure had been fully explained to all participants. Two subjects were discarded due to the failure to acquire reliable resting-state data; therefore, 16 subjects (11 males, age 21–25 years, mean 23.45 years) were included in the subsequent analyses. None of them had a history of neurological or psychiatric disorders and no current use of psychoactive medications.

### 2.2. Experimental procedures

This study consisted of an eyes-closed resting-state EEG recording with a 5 min duration and an 8.5 min long UG task. During the whole EEG data recording, subjects were consistently instructed to relax and refrain from extensive head motion. Each subject was told to be the responder during the

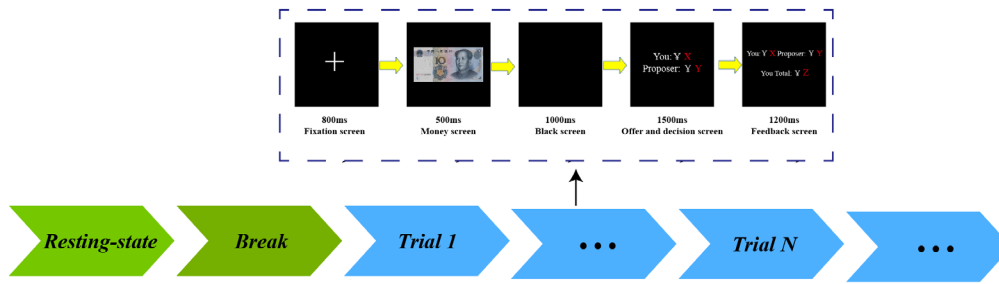


**Figure 1.** The UG task procedures and the timeline of a UG task trial.

UG task and played with another subject, the proposer, seated in another laboratory. During the UG task, subjects would decide whether to accept or reject the offer proposed by the proposer. If they accepted this offer, they were required to press the ‘1’ key on a standard keyboard; both the responder and the proposer would then receive the money assigned by the proposer; if the responder rejected the offer, however, they need to press the ‘3’ key on the keyboard, and consequently, both players earned nothing. The detailed UG task procedures are displayed in figure 1 and further depicted as follows.

The entire UG task lasted 8.5 mins. Before the UG, subjects were given a test to ensure their understanding of the task rule. In the UG task, subjects received 90 offers that were randomly presented on the computer screen and equally divided into three categories: fair (¥5: ¥5), moderately unfair (¥3: ¥7), and extremely unfair (¥1: ¥9). Every UG trial lasted for a total of 5 s. A fixation cross-hair first appeared and lasted for 800ms, followed by a 500 ms presentation of the money that was to be split. After a black screen with a duration of 1000ms, a random offer was presented for 1500ms. Once they noticed this proposed offer, subjects were required to make their decision (i.e. acceptance or rejection) on the offer. In the next feedback screen, the amount of money that two players received from that offer and his/her cumulative amount of winnings were presented for a duration of 1200ms. To eliminate the effect of fatigue on decision-making, every 30 UG trials the subjects were given a duration of 30s break.

### 2.3. EEG data recording

Subjects were seated in an electrically shielded and light-attenuated room. EEG data sets were recorded by 64 Ag/AgCl electrodes that were positioned in compliance with the 10/20 international electrode placement system (ASA-Lab Amplifier, ANT Neuro). The predefined online parameters of data recording were a 500 Hz sampling rate and 0.01–70 Hz online bandpass filtering. The electrodes CPZ and AFZ served as the reference and ground, respectively. The electrooculogram was recorded using an extra channel that was positioned above the left eye to monitor eye movements. For all electrodes, the impedance was kept below 5 K $\Omega$  during the EEG recording.

### 2.4. Resting-state EEG data analysis

In this study, resting-state EEG data sets were used to build the corresponding resting-state EEG networks, which were carried out using MATLAB v2014a (The MathWorks Inc.), and the analysis procedure is presented in figure 2. Detailed information regarding the data processing is depicted in the following sections.

**2.4.1. EEG data preprocessing.** Resting-state data sets were preprocessed with multiple procedures, including averaging-referencing, 0–45 Hz lowpass filtering, 5 s data segmentation, and artifact trial removal ( $\pm 60 \mu\text{V}$  as the threshold). After EEG data preprocessing, the range of valid segments for all subjects was  $39 \pm 13$ .

**2.4.2. Resting-state EEG network.** The volume conduction means that the nearby electrodes acquire a similar contribution from cortical sources and capture a similar activity. In our present study, to reduce the effect of volume conduction, following the procedure in related studies (Srinivasan *et al* 1998, Qin *et al* 2010, Tian and Yao 2013, Xu *et al* 2014, Li *et al* 2016) 21 canonical electrodes (i.e. FP1, FPz, FP2, F7, F3, Fz, F4, F8, T7, C3, Cz, C4, T8, P7, P3, Pz, P4, P8, O1, O2, Oz) of the 64 channels in the 10–20 system were used to construct the brain network. Various metrics, such as phase lock value (PLV), correlation, coherence (COH), entropy, etc, can be used to measure the interactions of different brain areas (Tian *et al* 2017b, Li *et al*, 2019a, 2019b), among which coherence is capable of capturing the coupling at specific frequency bands (Thatcher *et al* 2005) and has been widely used to analyze synchrony-defined cortical neuronal assemblies in the frequency domain. Moreover, various previous studies have shown that the relationship between brain network connectivity and cognition functions (i.e. attention, motor imagery) could be evaluated efficiently by coherence analysis (Zhang *et al* 2015, Li *et al* 2018b). In this study, we adopted frequency-specific COH to denote the linkage strength between two network nodes. This represents the linear relationship at a specific frequency between two signals,  $X(t)$  and  $Y(t)$ , based on their cross-spectrum, which is defined as

$$C_{XY}(f) = |R_{XY}(f)|^2 = \frac{|P_{XY}(f)|^2}{P_{XX}(f)P_{YY}(f)} \quad (1)$$

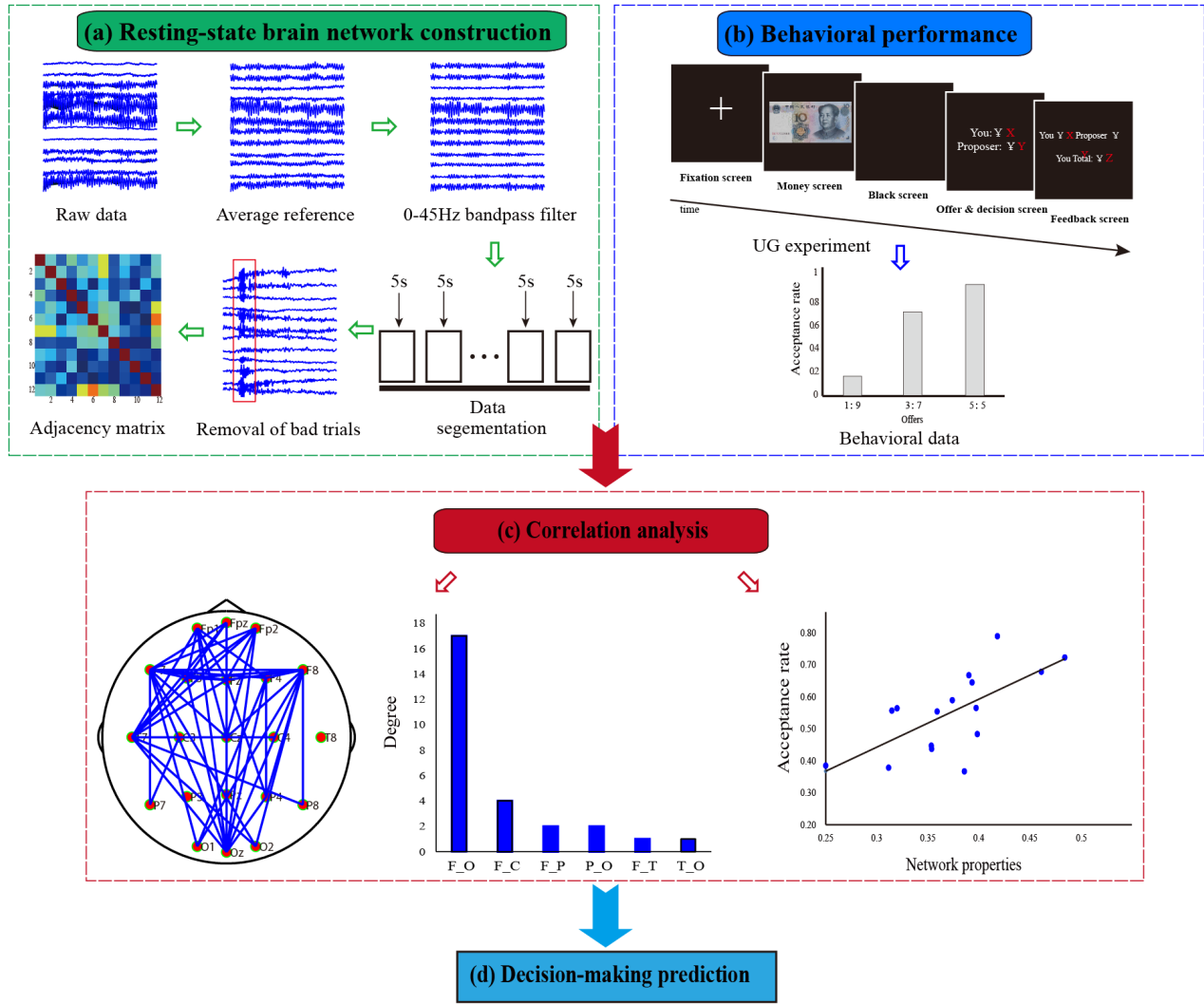


**Figure 2.** Analysis procedures for behavioral and resting-state data sets in the UG task. (a) Resting-state brain network construction, (b) behavioral performance (i.e. acceptance rate) estimation, (c) correlation analysis, and (d) decision-making prediction.

where  $C_{XY}(f)$  and  $R_{XY}(f)$  are the coherence and complex correlation coefficient between  $X(t)$  and  $Y(t)$  at frequency  $f$ , respectively.  $P_{XY}(f)$  is the cross-spectrum of  $X(t)$  and  $Y(t)$  at frequency  $f$ ,  $P_{XX}(f)$  and  $P_{YY}(f)$  represent the corresponding auto-spectrum at frequency  $f$ . These measurements of spectral density were calculated using the fast Fourier transform. The  $C_{XY}(f)$  for each frequency bin  $f$  is obtained by squaring the magnitude of the complex correlation coefficient  $R$ , which returns a real value within the range of [0, 1]. Based on 5 s segments, we then constructed the related EEG networks in five conventional EEG frequency bands, i.e. delta (0–3 Hz), theta (4–7 Hz), alpha (8–13 Hz), beta (14–30 Hz), and gamma (30–45 Hz) (Dasdemir *et al* 2017, Mumtaz *et al* 2017). For each specific band, the  $21 \times 21$  weighted adjacency (connectivity) matrix of the EEG network was obtained by averaging  $C_{XY}$  within the corresponding frequency range.

Based on graph theory, the resting-state network indexes were calculated after the weighted network was constructed. The clustering coefficient ( $C$ ), global efficiency ( $Ge$ ), local efficiency ( $Le$ ), and characteristic path length ( $L$ ) are four network properties that describe the ability of the resting-state

network to process information. For this study, these four weighted network properties were formulated using the following definitions and calculated by the brain connectivity toolbox (BCT, [www.nitrc.org/projects/bct/](http://www.nitrc.org/projects/bct/)) (Rubinov and Sporns 2010):

$$C = \frac{1}{N} \sum_{i \in \theta} \frac{\sum_{j,l \in \theta} (C_{ij} C_{il} C_{jl})^{1/3}}{\sum_{j \in w_{ij}} (\sum_{j \in \theta} C_{ij} - 1)} \quad (2)$$

$$Le = \frac{1}{N} \sum_{i \in \theta} \frac{\sum_{j,l \in \theta, j \neq i} (C_{ij} C_{il} [d_{jl}(\theta_i)]^{-1})^{1/3}}{\sum_{j \in \theta} C_{ij} (\sum_{j \in \theta} C_{ij} - 1)} \quad (3)$$

Here,  $C_{ij}$  is the connection strength between node  $i$  and  $j$ .  $N$  is the node number, and  $\theta$  is the set of all nodes of the resting-state network.  $C$  is defined as the fraction of triangles around an individual network node.  $Le$  is the average efficiency of the local subgraphs. Both  $C$  and  $Le$  are related to the estimation of the potential for functional segregation between brain lobes and reflect the local information processing capacity of the brain networks.



$$G_e = \frac{1}{N} \sum_{i \in \theta} \frac{\sum_{j \in \theta, j \neq i} d_{ij}^{-1}}{N-1} \quad (4)$$

$$L = \frac{1}{N} \sum_{i \in \theta} L_i = \frac{1}{N} \sum_{i \in \theta} \frac{\sum_{j \in \theta, j \neq i} d_{ij}}{N-1} \quad (5)$$

where  $G_e$  is the average efficiency of the related brain network and  $L$  is the mean value of the shortest path length between all pairs of network nodes. They are applied to estimate the potential for functional integration among brain areas. Additionally, they are defined as the efficiency of global information processing in brain networks.

### 2.5. Acceptance rate prediction based on multiple linear regression model

In this study, the four resting-state network properties (i.e.  $C$ ,  $G_e$ ,  $Le$ , and  $L$ ) were used as the variables in the multiple linear regression model for building a prediction model. The corresponding prediction model is as follows:

$$AR = \beta_0 + \beta_1 C + \beta_2 G_e + \beta_3 Le + \beta_4 L + \varepsilon \quad (6)$$

where  $AR$  denotes the acceptance rate in the UG task,  $\beta_0 \dots \beta_4$  denote the regression coefficients of the four network properties, and  $\varepsilon$  denotes the error term.

The leave-one-out cross-validation strategy was used to predict the acceptance rate of the individuals (Xu et al 2010, Zhang et al 2016, Tian et al 2017b). For  $n$  samples, in each leave-one-out cross validation,  $n-1$  samples were used for training, and the remaining sample was used for testing. The regression coefficient for each variable was estimated to build a prediction model for current  $n-1$  samples, which can then be used to predict the acceptance rate of an individual in the test set. This procedure was repeated  $n$  times until all  $n$  samples served as a testing set for one time.

To quantitatively measure the prediction performance, we first acquired the correlation coefficient between the actual and predicted acceptance rates by performing Person's correlation analysis. We further used the root mean square error (RMSE) to measure the prediction error:

$$RMSE = \sqrt{\frac{1}{N} \sum_{t=1}^N (X_t - Y_t)^2} \quad (7)$$

where  $N$  is the number of samples and  $X$  and  $Y$  correspond to the observed and predicted acceptance rates, respectively. Obviously, a smaller RMSE corresponds to a better prediction.

### 2.6. Statistical analysis

This work includes calculation of the correlation between network and subject decision-making behavior and analysis of the difference between the high- and low-acceptance groups (LAG). To explore the relationship between the acceptance rates and resting-state EEG network topology linkages and properties, Pearson's correlation with a false discovery rate

(FDR) correction was adopted. In addition to the correlation analysis, an independent-samples  $t$ -test with FDR correction was used to quantify the differences between the high-acceptance group and the low-acceptance group.

## 3. Results

### 3.1. Network topology correlated with decision-making

Figure 3 illustrates the significant network topologies that were demonstrated to be related to the acceptance rates in the UG task for five EEG bands. When investigating the potential correlation between network topology and acceptance rate, only the long-range frontal-occipital linkages of the resting-state brain network in the alpha band were found to be significantly correlated with acceptance rate ( $p < 0.05$ , FDR corrected).

### 3.2. Relationships between acceptance rates and resting-state network properties

We then explored the potential relationships between acceptance rates and the resting-state network properties ( $C$ ,  $L$ ,  $G_e$ , and  $Le$ ) in the five frequency bands (i.e. delta, theta, alpha, beta and gamma). As shown in table 1, in the alpha band,  $C$  ( $r = 0.681$ ,  $p = 0.004$ ),  $G_e$  ( $r = 0.676$ ,  $p = 0.004$ ), and  $Le$  ( $r = 0.683$ ,  $p = 0.004$ ) were demonstrated to be significantly positively correlated with acceptance rates, while  $L$  was negatively correlated with acceptance rates ( $r = -0.686$ ,  $p = 0.003$ ). There was no significant relationship between the acceptance rates and resting-state network properties in the other four frequency bands ( $p > 0.05$ ). Thus, figure 4 displays the scatter plots between both variables in the alpha band.

### 3.3. Differential network topologies between high- and low-acceptance groups

According to the acceptance rates across subjects, all sixteen subjects were divided into two groups, i.e. a high-acceptance group (HAG, eight subjects) and a low-acceptance group (LAG, eight subjects), to explore the underlying resting-state network differences by using an independent-sample  $t$ -test. The differential resting-state network topology in the alpha frequency band illustrated in figure 5 exhibited stronger frontal-occipital linkages for the HAG subjects compared to the LAG subjects ( $p < 0.05$ , FDR corrected). There were no differences revealed for the resting-state network in the other four frequency bands between HAG and LAG ( $p > 0.05$ ). To further reveal the spatial distribution of the different topology patterns, we separated the electrodes into frontal (FP1, FPz, FP2, F7, F3, Fz, F4, F8), occipital (O1, Oz, O2), central (C3, Cz, C4), parietal (P3, Pz, P4), and temporal (T7, T8, P7, P8) groups following the spatial positions of electrodes. Then, we calculated the sum of linkage strengths between any two pairs of the five brain areas to quantitatively differentiate the different connection patterns among them. The bar plot in figure 5(b) shows the corresponding sum of linkage strengths

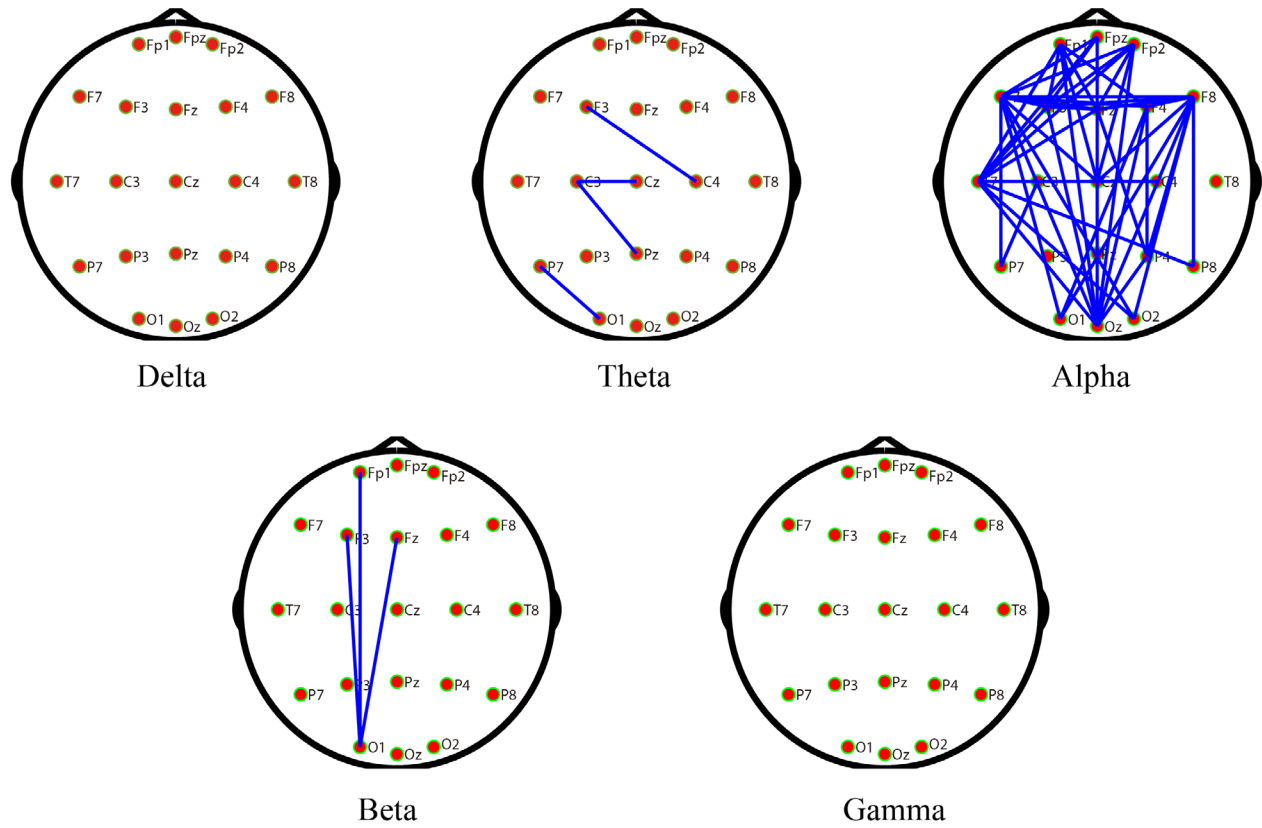


**Figure 3.** The network topologies significantly related to the acceptance rate within five EEG bands in the UG task. The blue solid lines represent the edges with significant correlations with acceptance rate ( $p < 0.05$ , FDR corrected).

**Table 1.** Correlation between acceptance rate and network properties within the five bands.

		<i>C</i>	<i>L</i>	<i>Ge</i>	<i>Le</i>
delta	<i>r</i>	0.346	−0.354	0.341	0.346
	<i>p</i>	0.189	0.179	0.197	0.190
theta	<i>r</i>	0.034	−0.062	0.080	0.048
	<i>p</i>	0.899	0.818	0.768	0.860
alpha	<i>r</i>	<b>0.681</b>	<b>−0.686</b>	<b>0.676</b>	<b>0.683</b>
	<i>p</i>	<b>0.004</b>	<b>0.003</b>	<b>0.004</b>	<b>0.004</b>
beta	<i>r</i>	0.501	−0.490	0.455	0.486
	<i>p</i>	0.050	0.055	0.08	0.057
gamma	<i>r</i>	0.204	−0.209	0.215	0.209
	<i>p</i>	0.448	0.437	0.423	0.438

for the five brain areas. Consistent with the differential network topology patterns in figures 5(a) and (b) clearly demonstrated that the dominated enhanced linkages are mainly those of the connections between frontal and occipital areas.

### 3.4. Acceptance rate prediction based on the resting-state network properties

Given that the resting-state network properties were highly correlated with the acceptance rates (figure 4), the network properties (*C*, *L*, *Ge*, and *Le*) may serve as features to predict individual acceptance rates in the UG task. Figure 6 illustrates the relationship between actual and predicted acceptance

rates, where the *X* and *Y* axes denote the predicted and actual acceptance rates, respectively. The corresponding Pearson's correlation coefficient was  $r = 0.58$  ( $P = 0.01$ ), and the RMSE was 10.24%.

## 4. Discussions

Previous studies have already demonstrated the relationship between decision-making behaviors and task-related brain activation (Calder *et al* 2001, Sanfey *et al* 2003, Van't Wout *et al* 2006), but whether resting-state brain connectivity is predictable for the decision response of the individual has not yet been probed. Given that the large-scale networks among various areas at resting-state are closely related to human cognition (Buschman and Miller 2007), and decision-making has also shown the importance of various neural networks, including the frontoparietal system (Paulus *et al* 2001), brain network analysis was adopted to investigate the potential relationship between brain network connectivity at resting-state and decision-making in the UG task. Our current work provides interesting evidence that links the resting-state brain network and UG task performance.

We found that the long-range frontal-occipital linkages in the resting-state network from the alpha band of the resting-state EEG were significantly correlated with the acceptance rate in the UG task. When resting-state EEG is recorded with eyes closed, it is characterized with predominantly alpha oscillations. Generally, the alpha rhythm may be a marker of

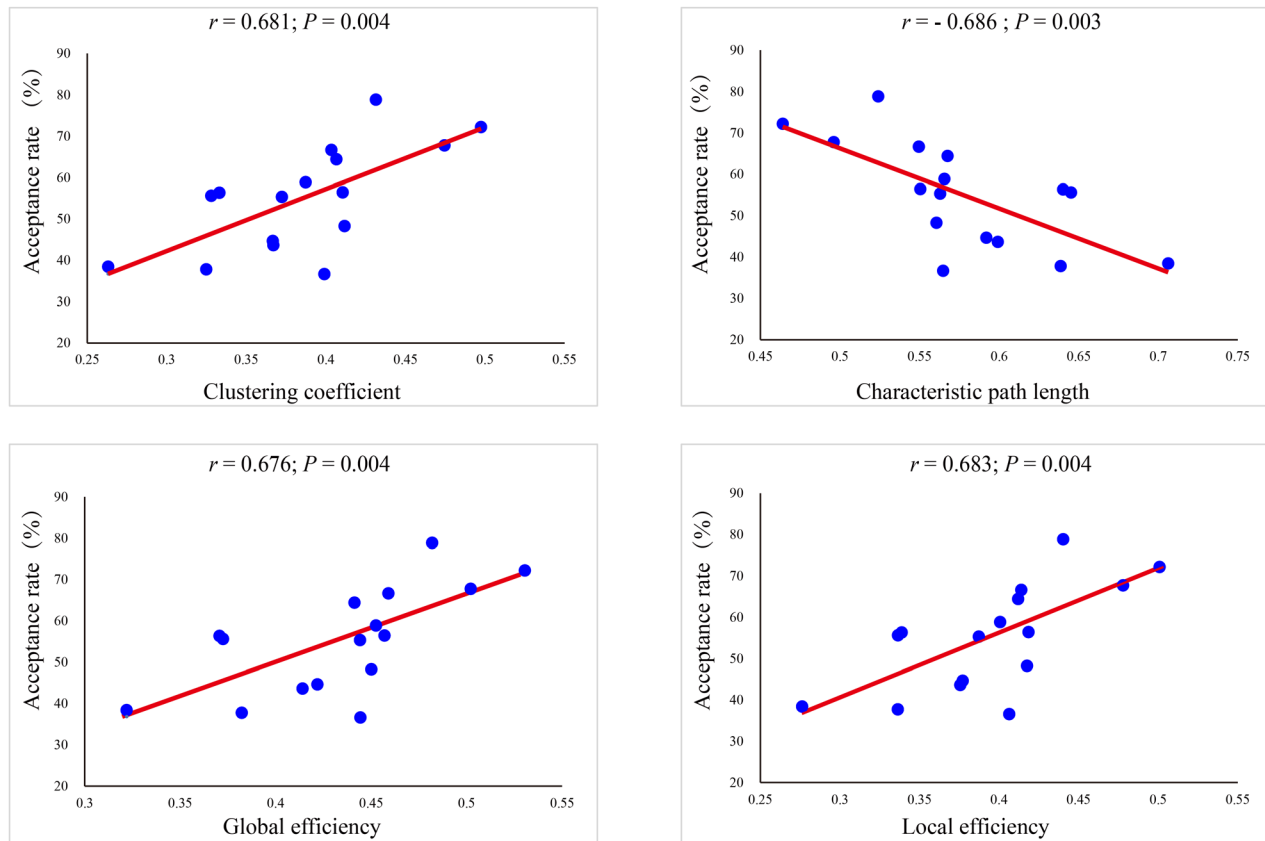


**Figure 4.** Relationships between the resting-state network properties and acceptance rates in the alpha band. In each subfigure, the red line is the fitted curve,  $r$  indicates the correlation coefficient, and  $p$  indicates the statistical significance level.

the individual's state of arousal and attention and is related to task performance, as shown by previous studies (Jann *et al* 2010, Klimesch 2012). The alpha band has been shown to be related to various cognitive features, such as working memory capacity (Clark and Veltmeyer 2004), information processing speed (Klimesch 1996), and inhibition (Klimesch 2012). Furthermore, the alpha band has also been found to be associated with attentional arousal as well as cognitive preparedness (Angelakis *et al* 2004). Therefore, the brain activity in the alpha band may preconfigure the attentional and cognitive resources that are crucial in the subsequent task and thereby index the potential capacity of the brain to efficiently process information during tasks (Zhang *et al* 2013). In essence, brain areas including the ventromedial prefrontal cortex and insula engage in decision-making by processing cognitive and emotional information (Critchley *et al* 2000, Polezzi *et al* 2008, Bartra *et al* 2013). In particular, the frontal lobe is considered to be related to executive control and goal maintenance in decision-making (Huerta and Kaas 1990, Munakata *et al* 2011). Moreover, the role of the prefrontal cortex in the neural network is that fundamental impulses are connected with self-interest, which is a deliberative processes in human decision-making (Henrich *et al* 2001). The occipital lobe plays an important role in visual recognition (Haxby *et al* 2000) that helps humans quickly identify the decision situation for subsequent choices. Actually, the high-level cognitive processes, such as attention, motor imagery, and creativity, are attributed to information exchange within a large-scale network (Li *et al*

2016, 2018a, Sun *et al* 2018). Decision-making involves the network topology spanning the frontal and occipital lobes, which engages the neural systems supporting value assessment, including external factors and internal factors and integrating information to make a decision. Our current study demonstrated a similar pattern (figure 3) wherein the resting-state frontal-occipital linkages were related to the UG task performance (i.e. acceptance rate).

Furthermore, we found that an increased acceptance rate was accompanied by an increased  $C$ ,  $Ge$ , and  $Le$  as well as a shorter  $L$ . Theoretically, the increased  $C$ ,  $Ge$ , and  $Le$  as well as the shorter  $L$  indicated an increase in the efficiency of information processing in the brain; here, figure 4 demonstrates that an efficient resting-state network corresponds to a high acceptance rate in the UG task. As far as we know, decision-making involves multiple cognitive processes, such as attention and working memory, that depend on the large-scale brain networks (Bressler and Menon 2010, Li *et al* 2015). Moreover, the uncertain condition involves more complex information processing (Polezzi *et al* 2008), and the rational decision is to accept them according to the goal of benefit maximization in economic game theory (Yamagishi *et al* 2009). Therefore, when the resting brain is working efficiently, it will provide a high potential to efficiently identify decision conditions and to make a rational decision in the UG task as well, which eventually contributes to a high acceptance rate in decision-making. Motivated by the close correlations between network properties and acceptance rates, multiple linear regression analysis

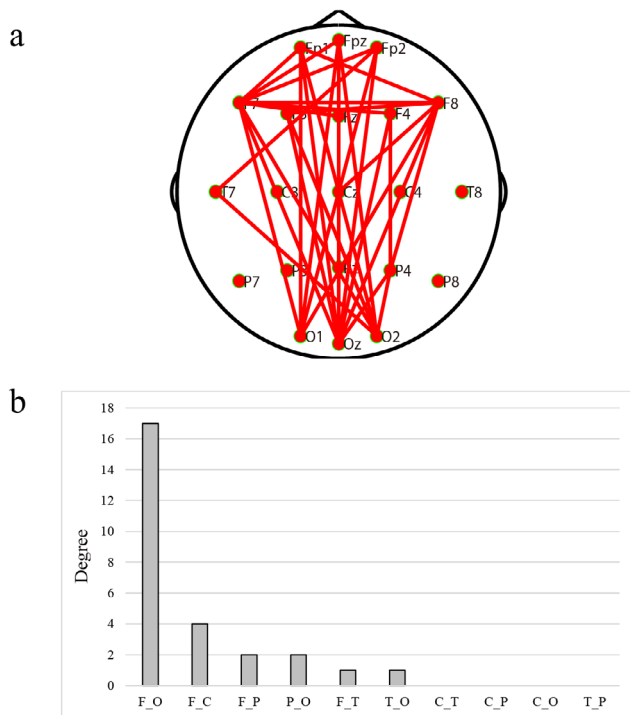


**Figure 5.** Differential resting-state network topology pattern between HAG and LAG in the alpha band. (a) Spatial topology pattern. The red solid lines denote the stronger network edges ( $p < 0.05$ , FDR corrected) of the HAG group compared to those of the LAG group. (b) Sum of linkage strengths in (a) between any two pairs of the five brain areas for HAG and LAG in the alpha band. F: Frontal; O: Occipital; P: Parietal; T: Temporal; C: Central.

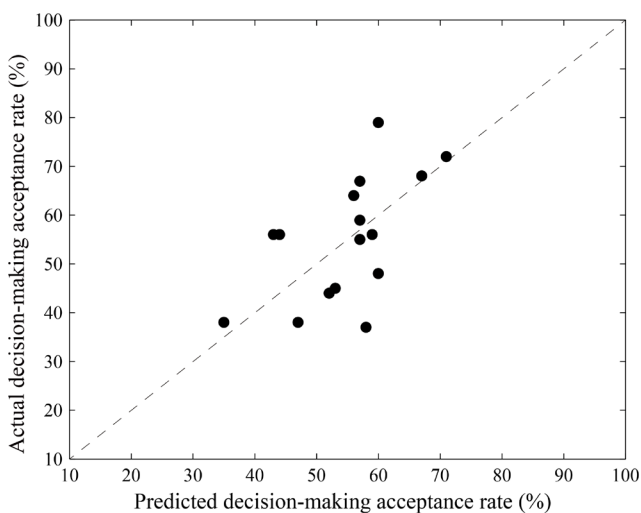


**Figure 6.** The relationship between predicted (X-axis) and actual (Y-axis) acceptance rate. The black filled circles denote the subjects.

was adopted to build a model to predict the decision acceptance rate. In figure 6, the dashed diagonal line indicates ideal prediction, and the black filled circles distributed along the diagonal line denote that the regression model estimated from the training set was capable of accurately predicting an individual's decision-making acceptance rate.

The relationship between the resting-state brain network and acceptance rate raised an issue of whether there is a

difference in the resting-state brain networks of high- and LAGs. In this study, we found stronger frontal-occipital linkages for the HAG subjects when compared to the LAG subjects. A previous study showed that when subjects accept the proposed offer, stronger activation was observed in the dorso-lateral prefrontal cortex (Sanfey *et al* 2003). Moreover, in a visual decision task, the decision-making activations usually initialize the parts of the visual cortex related to visual recognition and object sensitivity and then spread to the prefrontal regions involved in assessing and making rational decisions (Pearson and Platt 2012, Dilks *et al* 2013). The stronger resting-state frontal-occipital pattern observed for individuals with high acceptance rates may infer that those subjects tended to make a rational decision (i.e. to accept the unfair offers), which may further support the positive correlations between the network efficiency and acceptance rates in figure 4.

In the present study, the networks were constructed at the scalp level, which may have been influenced by the volume conduction effect (Schoffelen 2009). Although we used the sparse 21 canonical electrodes of the 10–20 EEG system to lower the effect of volume conduction, the technique of the construction of networks at the cortical level known as EEG source connectivity is another important solution, which may be more competitive in constructing a more reliable EEG network (O'Neill *et al* 2015, 2017, Kabbara *et al* 2017, 2018, Hassan and Wendling 2018). In a future work, we will construct EEG networks at the source level to further prove the association between resting-state functional connectivity and decision-making, as well as other cognition processes, such as working memory and attention, etc.

## 5. Conclusion

In conclusion, we found that resting-state frontal-occipital connectivity played a crucial role in decision-making, where an efficient brain at rest indicated that an individual was inclined to make rational decisions. By using resting-state network properties as the variables in a multiple linear regression model, we could achieve a relatively high correlation coefficient of 0.58 between the actual and predicted acceptance rate, along with a relatively small RMSE of 10.24%. Together, these results deepened our understanding of decision-making from the perspective of resting-state brain networks and might provide a potential physiological biomarker to predict responses in decision-making.

## Acknowledgments



This work was supported by the National Key Research and Development Plan of China (#2017YFB1002501), the National Natural Science Foundation of China (#81771925, #61603344, and #71601136).

## ORCID iDs

Yajing Si <https://orcid.org/0000-0003-0294-2352>

Fali Li <https://orcid.org/0000-0002-2450-4591>



Tao Zhang  <https://orcid.org/0000-0002-2891-4213>  
 Feng Wan  <https://orcid.org/0000-0002-9359-0737>

## References

- Amodio D M and Frith C D 2006 Meeting of minds: the medial frontal cortex and social cognition *Nat. Rev. Neurosci.* **7** 268
- Angelakis E, Lubar J F, Stathopoulou S and Kounios J 2004 Peak alpha frequency: an electroencephalographic measure of cognitive preparedness *Clin. Neurophysiol.* **115** 887–97
- Bartra O, McGuire J T and Kable J W 2013 The valuation system: a coordinate-based meta-analysis of BOLD fMRI experiments examining neural correlates of subjective value *NeuroImage* **76** 412–27
- Basten U, Biele G, Heekeren H R and Fiebach C J 2010 How the brain integrates costs and benefits during decision making *Proc. Natl Acad. Sci. USA* **107** 21767–72
- Bressler S L and Menon V 2010 Large-scale brain networks in cognition: emerging methods and principles *Trends Cogn. Sci.* **14** 277–90
- Brokaw K, Tishler W, Manceor S, Hamilton K, Gaulden A, Parr E and Wamsley E J 2016 Resting state EEG correlates of memory consolidation *Neurobiol. Learn. Mem.* **130** 17–25
- Buschman T J and Miller E K 2007 Top-down versus bottom-up control of attention in the prefrontal and posterior parietal cortices *Science* **315** 1860–2
- Calder A J, Lawrence A D and Young A W 2001 Neuropsychology of fear and loathing *Nat. Rev. Neurosci.* **2** 352–63
- Clark C and Veltmeyer M D 2004 Spontaneous alpha peak frequency predicts working memory performance across the age span *Int. J. Psychophysiol.* **53** 1–9
- Critchley H D, Elliott R, Mathias C J and Dolan R J 2000 Neural activity relating to generation and representation of galvanic skin conductance responses: a functional magnetic resonance imaging study *J. Neurosci.* **20** 3033–40
- Dasdemir Y, Yildirim E and Yildirim S 2017 Analysis of functional brain connections for positive-negative emotions using phase locking value *Cogn. Neurodyn.* **11** 487–500
- Dilks D D, Julian J B, Paunov A M and Kanwisher N 2013 The occipital place area is causally and selectively involved in scene perception *J. Neurosci.* **33** 1331–6
- Dixon M L, Andrews-Hanna J R, Spreng R N, Irving Z C, Mills C, Girn M and Christoff K 2017 Interactions between the default network and dorsal attention network vary across default subsystems, time, and cognitive states *NeuroImage* **147** 632–49
- Dodds C M, Morein-Zamir S and Robbins T W 2010 Dissociating inhibition, attention, and response control in the frontoparietal network using functional magnetic resonance imaging *Cereb Cortex* **21** 1155–65
- Falahpour M, Chang C, Wong C W and Liu T T 2018 Template-based prediction of vigilance fluctuations in resting-state fMRI *NeuroImage* **174** 317–27
- Hassan M and Wendling F 2018 Electroencephalography source connectivity: toward high time/space resolution brain networks *IEEE Signal Proc. Mag.* **35** 1–25
- Haxby J V, Hoffman E A and Gobbini M I 2000 The distributed human neural system for face perception *Trends Cogn. Sci.* **4** 223–33
- Henrich J, Boyd R, Bowles S, Camerer C, Fehr E, Gintis H and McElreath R 2001 In search of homo economicus: behavioral experiments in 15 small-scale societies *Am. Econ. Rev.* **91** 73–8
- Horat S K, Prévot A, Richiardi J, Herrmann F R, Favre G, Merlo M C G and Missonnier P 2017 Differences in social decision-making between proposers and responders during the Ultimatum Game: an EEG study *Frontiers Integr. Neurosci.* **11** 13
- Huerta M F and Kaas J H 1990 Supplementary eye field as defined by intracortical microstimulation: connections in macaques *J. Comp. Neurol.* **293** 299–330
- Jann K, Koenig T, Dierks T, Boesch C and Federspiel A 2010 Association of individual resting state EEG alpha frequency and cerebral blood flow *NeuroImage* **51** 365–72
- Kabbara A, Eid H, El Falou W, Khalil M, Wendling F and Hassan M 2018 Reduced integration and improved segregation of functional brain networks in Alzheimer's disease *J. Neural Eng.* **15** 026023
- Kabbara A, El Falou W, Khalil M, Wendling F and Hassan M 2017 The dynamic functional core network of the human brain at rest *Sci. Rep.* **7** 2936
- Kaltwasser L, Hildebrandt A, Wilhelm O and Sommer W 2016 Behavioral and neuronal determinants of negative reciprocity in the ultimatum game *Soc. Cogn. Affect. Neurosci.* **11** 1608–17
- Kim S and Lee D 2011 Prefrontal cortex and impulsive decision making *Biol. Psychiatry* **69** 1140–6
- Kirk U, Downar J and Montague R 2011 Interoception drives increased rational decision-making in meditators playing the ultimatum game *Frontiers Neurosci.* **5** 49
- Klimesch W 1996 Memory processes, brain oscillations and EEG synchronization *Int. J. Psychophysiol.* **24** 61–100
- Klimesch W 2012 Alpha-band oscillations, attention, and controlled access to stored information *Trends Cogn. Sci.* **16** 606–17
- Kounios J, Fleck J I, Green D L, Payne L, Stevenson J L, Bowden E M and Jung-Beeman M 2008 The origins of insight in resting-state brain activity *Neuropsychologia* **46** 281–91
- Krain A L, Wilson A M, Arbuckle R, Castellanos F X and Milham M P 2006 Distinct neural mechanisms of risk and ambiguity: a meta-analysis of decision-making *NeuroImage* **32** 477–84
- Lamichhane B, Adhikari B M and Dhamala M 2016 The activity in the anterior insulae is modulated by perceptual decision-making difficulty *Neuroscience* **327** 79–94
- Li F et al 2016 The time-varying networks in P300: a task-evoked EEG study *IEEE Trans. Neural Syst. Rehabil. Eng.* **24** 725–33
- Li F et al 2018a The Dynamic brain networks of motor imagery: time-varying causality analysis of scalp EEG *Int. J. Neural Syst.* **19** 1850016
- Li F et al 2019a Transition of brain networks from an interictal to a preictal state preceding a seizure revealed by scalp EEG network analysis *Cogn. Neurodyn.* **13** 175–81
- Li F et al 2015 Relationships between the resting-state network and the P3: evidence from a scalp EEG study *Sci. Rep.* **5** 15129
- Li F, Yi C, Jiang L, Peng W, Si Y, Zhang T, Zhang R, Yao D, Zhang Y and Xu P 2018b Brain network reconfiguration during motor imagery revealed by a large-scale network analysis of scalp EEG *Brain Topogr.* **32** 304–14
- Li N, Ma N, Liu Y, He X S, Sun D L, Fu X M, Zhang X, Han S and Zhang D R 2013 Resting-state functional connectivity predicts impulsivity in economic decision-making *J. Neurosci.* **33** 4886–95
- Li P et al 2019b EEG based emotion recognition by combining functional connectivity network and local activations *IEEE Trans. Biomed. Eng.* **66** 2869–81
- Mumtaz W, Vuong P L, Xia L, Malik A S and Rashid R B A 2017 An EEG-based machine learning method to screen alcohol use disorder *Cogn. Neurodyn.* **11** 161–71
- Munakata Y, Herd S A, Chatham C H, Depue B E, Banich M T and O'reilly R C 2011 A unified framework for inhibitory control *Trends Cogn. Sci.* **15** 453–9
- Neuberta F X, Marsa R B, Salleta J and Rushwortha M F 2015 Connectivity reveals relationship of brain areas for reward-guided learning and decision making in human and monkey frontal cortex *Proc. Natl Acad. Sci. USA* **112** E2695–704
- Northoff G, Qin P and Nakao T 2010 Rest-stimulus interaction in the brain: a review *Trends Cogn. Sci.* **33** 277–84

- O'Neill G C, Bauer M, Woolrich M W, Morris P G, Barnes G R and Brookes M J 2015 Dynamic recruitment of resting state sub-networks *NeuroImage* **115** 85–95
- O'Neill G C, Tewarie P K, Colclough G L, Gascoyne L E, Hunt B A E, Morris P G, Woolrich M W and Brookes M J 2017 Measurement of dynamic task related functional networks using MEG *NeuroImage* **146** 667–78
- Paulus M P, Hozack N, Zauscher B, McDowell J E, Frank L, Brown G G and Braff D L 2001 Prefrontal, parietal, and temporal cortex networks underlie decision-making in the presence of uncertainty *NeuroImage* **13** 91–100
- Pearson J and Platt M L 2012 Dynamic decision making in the brain *Nat. Neurosci.* **15** 341–2
- Peterburs J, Voegler R, Liepelt R, Schulze A, Wilhelm S, Ocklenburg S and Straube T 2017 Processing of fair and unfair offers in the ultimatum game under social observation *Sci. Rep.* **7** 44062
- Polezzi D, Daum I, Rubaltelli E, Lotto L, Civali C, Sartori G and Rumiati R 2008 Mentalizing in economic decision-making *Behav. Brain Res.* **190** 218–23
- Qin Y, Xu P and Yao D 2010 A comparative study of different references for EEG default mode network: the use of the infinity reference *Clin. Neurophysiol.* **121** 1981–91
- Rubinov M and Sporns O 2010 Complex network measures of brain connectivity: uses and interpretations *NeuroImage* **52** 1059–69
- Sanfey A G, Rilling J K, Aronson J A, Nystrom L E and Cohen J D 2003 The neural basis of economic decision-making in the ultimatum game *Science* **300** 1755–8
- Schoffelen J M and Gross J 2009 Source connectivity analysis with MEG and EEG *Hum. Brain Mapp.* **30** 1857–65
- Shao R, Sun D and Lee T M 2016 The interaction of perceived control and Gambler's fallacy in risky decision making: an fMRI study *Hum. Brain Mapp.* **37** 1218
- Si Y et al 2018 Different decision-making responses occupy different brain networks for information processing: a study based on EEG and TMS *Cereb. Cortex* **29** 4119–29
- Srinivasan R, Nunez P L and Silberstein R B 1998 Spatial filtering and neocortical dynamics: estimates of EEG coherence *IEEE Trans. Biomed. Eng.* **45** 814–26
- Sun J et al 2018 Verbal creativity correlates with the temporal variability of brain networks during the resting state *Cereb. Cortex* **29** 1047–58
- Suzuki S, Harasawa N, Ueno K, Gardner J L, Ichinohe N, Haruno M, Cheng K and Nakahara H 2012 Learning to simulate others' decisions *Neuron* **74** 1125–37
- Thatcher R W, North D and Biver C 2005 EEG and intelligence: relations between EEG coherence, EEG phase delay and power *Clin Neurophysiol* **116** 2129–41
- Tian Y and Yao D 2013 Why do we need to use a zero reference? Reference influences on the ERPs of audiovisual effects *Psychophysiology* **50** 1282–90
- Tian Y, Yang L, Chen S, Guo D, Ding Z, Tam K Y and Yao D 2017a Causal interactions in resting-state networks predict perceived loneliness *PLoS One* **12** e0177443
- Tian Y, Zhang H, Xu W, Zhang H, Yang L, Zheng S and Shi Y 2017b Spectral entropy can predict changes of working memory performance reduced by short-time training in the delayed-match-to-sample task *Frontiers Hum. Neurosci.* **11** 437
- Tremblay S, Sharika K M and Platt M L 2017 Social decision-making and the brain: a comparative perspective *Trends Cogn. Sci.* **21** 256–76
- Van't Wout M, Kahn R S, Sanfey A G and Aleman A 2006 Affective state and decision-making in the ultimatum game *Exp. Brain Res.* **169** 564–8
- Wang G, Li J, Li Z, Wei M and Li S 2016 Medial frontal negativity reflects advantageous inequality aversion of proposers in the ultimatum game: an ERP study *Brain Res.* **1639** 38–46
- Wang Y, Zhang Z, Bai L, Lin C, Osinsky R and Hewig J 2017 Ingroup/outgroup membership modulates fairness consideration: neural signatures from ERPs and EEG oscillations *Sci. Rep.* **7** 39827
- Waskom M L, Frank M C and Wagner A D 2016 Adaptive engagement of cognitive control in context-dependent decision making *Cereb. Cortex* **27** 1270–84
- Xu P, Kaspruwicz M, Bergsneider M and Hu X 2010 Improved noninvasive intracranial pressure assessment with nonlinear kernel regression *IEEE Trans. Inf. Technol. B* **14** 971–8
- Xu P, Xiong X, Xue Q, Li P, Zhang R, Wang Z, Valdes-Sosa P A, Wang Y and Yao D 2014 Differentiating between psychogenic nonepileptic seizures and epilepsy based on common spatial pattern of weighted EEG resting networks *IEEE Trans. Biomed. Eng.* **61** 1747–55
- Yamagishi T, Horita Y, Takagishi H, Shinada M, Tanida S and Cook K S 2009 The private rejection of unfair offers and emotional commitment *Proc. Natl Acad. Sci. USA* **106** 11520–3
- Zhang R, Yao D, Valdés-Sosa P A, Li F, Li P, Zhang T, Ma T, Li Y and Xu P 2015 Efficient resting-state EEG network facilitates motor imagery performance *J. Neural Eng.* **12** 066024
- Zhang S, Wu W, Huang G, Liu Z, Guo S, Yang J and Wang K 2014 Resting-state connectivity in the default mode network and insula during experimental low back pain *Neural Regen. Res.* **9** 135
- Zhang T 2018 Reconfiguration patterns of large-scale brain networks in motor imagery *Brain Struct. Funct.* **224** 553–66
- Zhang T et al 2016 Structural and functional correlates of motor imagery BCI performance: insights from the patterns of fronto-parietal attention network *NeuroImage* **134** 475–85
- Zhang Y, Xu P, Guo D and Yao D 2013 Prediction of SSVEP-based BCI performance by the resting-state EEG network *J. Neural Eng.* **10** 066017